Supplementary materials for

Mutual 3:1 Subharmonic Synchronization in a Micromachined Silicon Disk Resonator

Parsa Taheri-Tehrani,[1] Andrea Guerrieri,[2] Martial Defoort,[1] Attilio Frangi,[2] and David A. Horsley[1]

[1]*Department of Mechanical and Aerospace Engineering, University of California, Davis, CA 95616, USA*

[2]*Department of Civil and Environmental Engineering, Politecnico di Milano, 20133 Milano, Italy*

The equations of motion of two resonance modes with non-dissipative, cubic nonlinear bidirectional coupling are:

$$\begin{aligned} \ddot{x}_1 + \Delta\omega_1\dot{x}_1 + \omega_1^2 x_1 &= k_1 x_1^3 + k_2 x_1^2 x_2 + k_3 x_1 x_2^2 + k_4 x_2^3 + \lambda_1 \\ \ddot{x}_2 + \Delta\omega_2\dot{x}_2 + \omega_2^2 x_2 &= k_5 x_1^3 + k_6 x_1^2 x_2 + k_7 x_1 x_2^2 + k_8 x_2^3 + \lambda_2 \end{aligned} \tag{S.1}$$

In these equations, x_1 and x_2 are the amplitudes of the first and second resonance modes with resonant frequencies of $\omega_1 = 2\pi f_1$ and $\omega_2 = 2\pi f_2$ respectively. $\Delta\omega_1 = \omega_1 / Q_1$ and $\Delta\omega_2 = \omega_2 / Q_2$ are the full width at half maximum (FWHM) bandwidths of the first and second resonance modes, respectively. λ_1 and λ_2 are external forces applied to the modes. The nonlinear stiffness terms k_1 and k_8 are cubic terms that result in Duffing nonlinearity in single DOF resonators, while k_2 through k_7 represent the cubic nonlinear coupling between the two modes. If k_2 through k_7 are zero, the equations represent two decoupled Duffing oscillators. As we are dealing with two oscillators that have a 3:1 frequency relationship, only the cubic nonlinear terms are included in the equations as these terms are the only ones that create third harmonics in the first-order approximation used here. These equations can be solved by a first-order approximation using a perturbation and multiple time-scales method with $x_1 = 1/2\, X_1 e^{i(\omega_1 t+\theta_1)} + 1/2\, X_1 e^{-i(\omega_1 t+\theta_1)}$, $x_2 = 1/2\, X_2 e^{i(\omega_2 t+\theta_2)} + 1/2\, X_2 e^{-i(\omega_2 t+\theta_2)}$, $\lambda_1 = 1/2\,\Lambda_1 e^{i(\Omega_1 t+\tau_1)} + 1/2\,\Lambda_1 e^{-i(\Omega_1 t+\tau_1)}$, and $\lambda_2 = 1/2\,\Lambda_2 e^{i(\Omega_2 t+\tau_2)} + 1/2\,\Lambda_2 e^{i(\Omega_2 t+\tau_2)}$, where X_1 and X_2 are the oscillation amplitudes, Λ_1 and Λ_2 are the forcing amplitudes, Ω_1 and Ω_2 are the forcing frequencies, and θ_1, θ_2, τ_1 and τ_2 represent the phase of each signal. The solution results in the following four amplitude and phase equations in the base harmonic of each mode:

$$
\begin{aligned}
8\omega_1\left(\frac{\Delta\omega_1}{2}X_1+\dot{X}_1\right)&=4\Lambda_1\sin(\gamma_1)+k_2X_2X_1^2\sin(\gamma_3)\\
8\omega_1X_1\dot{\theta}_1&=-2k_3X_1X_2^2-4\Lambda_1\cos(\gamma_1)-3k_1X_1^3-k_2X_1^2X_2\cos(\gamma_3)\\
8\omega_2\left(\frac{\Delta\omega_2}{2}X_2+\dot{X}_2\right)&=4\Lambda_2\sin(\gamma_2)-k_5X_1^3\sin(\gamma_3)\\
8\omega_2X_2\dot{\theta}_2&=-2k_6X_2X_1^2-4\Lambda_2\cos(\gamma_2)-3k_8X_2^3-k_5X_1^3\cos(\gamma_3)
\end{aligned}
\tag{S.2}
$$

These equations are four ordinary nonlinear differential equations. The first two are the amplitude and phase equations for the first mode, and the third and fourth equations are the amplitude and phase equations for the second mode. k_2, k_3, k_5, and k_6 are coupling terms that appear in the solution and result in energy exchange between the two modes. k_2, k_5 and are the terms that result in internal resonance and consequently synchronization. The variables defined in the letter are listed here:

$$
\begin{aligned}
\mathrm{K}_1=\frac{\Lambda_1}{2\omega_1},\ \delta_1=\frac{k_2}{8\omega_1},\ \alpha_1=\frac{3k_1}{8\omega_1},\ \beta_1=\frac{k_3}{4\omega_1}\\
\mathrm{K}_2=\frac{\Lambda_2}{2\omega_2},\ \delta_2=\frac{k_5}{8\omega_2},\ \alpha_2=\frac{3k_8}{8\omega_2},\ \beta_2=\frac{k_6}{4\omega_2}
\end{aligned}
\tag{S.3}
$$

Also in these equations:

$$
\begin{aligned}
\gamma_1&=\sigma_1t+\tau_1-\theta_1\\
\gamma_2&=\sigma_2t+\tau_2-\theta_2\\
\gamma_3&=\sigma_3t+\theta_2-3\theta_1
\end{aligned}
\tag{S.4}
$$

where σ_1 and σ_2 are the frequency detuning parameters of the forces applied to the first and second modes: $\Omega_1=\sigma_1+\omega_1$ and $\Omega_2=\sigma_2+\omega_2$. By having γ_1 and γ_2 fixed at 90º, the phase of each force input is fixed to excite the corresponding mode at the frequency that maximizes the vibration amplitude; in our experiments, the PLL provides this phase control. The resulting values of σ_1 and σ_2 in the numerical solution depend on the A-*f* dependence of each mode due to the Duffing nonlinear stiffness terms, k_1 and k_8 (also known as the backbone curve of the Duffing oscillator). By modeling the PLL in this manner, nonlinear damping terms (*e.g.* van der Pol self-sustained oscillators) are avoided, resulting in a more realistic oscillator model, and the PLL dynamics are omitted, making the model depend only on the micromechanical resonator's dynamics. σ_3 is the frequency detuning parameter between the two resonance modes: $\omega_2=\sigma_3+3\omega_1$. This detuning parameter is effectively the same parameter that we adjust through the

tuning voltage in our experiments. When synchronized, the phase difference between the two resonances (γ_3) reaches a stable, constant value.

Among all the terms in Eq. S.2 and S.3, $\alpha_1 X_1^2$, $\beta_1 X_2^2$, $\alpha_2 X_2^2$, and $\beta_2 X_1^2$ are easily measurable. By tracking the frequencies f_1 and f_2 as the amplitude of X_1 is increased, one can measure $\alpha_1 X_1^2$ and $\beta_2 X_1^2$, where $\alpha_1 X_1^2$ is the change in frequency of f_1 (known as Duffing A-f dependence) and $\beta_2 X_1^2$ is the change in frequency of f_2 (known as coupling A-f dependence). Similarly, by changing the amplitude of f_2 and tracking the frequency of f_1 and f_2, one can measure $\beta_1 X_2^2$ and $\alpha_2 X_2^2$. Measured data for these parameters are presented in Fig. S.1.

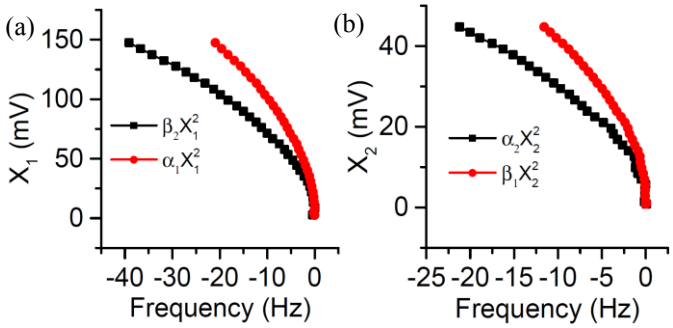

Fig. S.1: Measured A-f dependence of the two modes due to Duffing nonlinearity and cubic nonlinear coupling.

Table S.1 lists the parameter values used in the simulations presented in Fig. 3 and Fig. 4 of the manuscript. The values of k_1, k_3, k_6, and k_8 are estimated from the measured frequency response. The values of k_2 and k_5 are adjusted to fit the measured synchronization range. The values of k_1, k_3, k_6, and k_8 do not change the synchronization range but they do shift the frequency of the maximum amplitude and affect the behavior of X_1, X_2, $\theta_2 - 3\theta_1$, and f_1 (Fig. 4). Using the values listed in Table S.1, the simulated data presented in Fig. 3 and Fig. 4 can be reproduced.

Table S.1: Simulation parameters

Parameter	Value	Units
$\Delta\omega_1$	$2\pi\cdot 20$	rad/s
$\Delta\omega_2$	$2\pi\cdot 14$	rad/s
k_1, k_8	$5\cdot 10^{22}$	$1/(m\cdot s)^2$
k_2, k_5	$1.39\cdot 10^{22}$	$1/(m\cdot s)^2$
k_3, k_6	$3\cdot 10^{22}$	$1/(m\cdot s)^2$
ω_1	$2\pi\cdot 278000$	rad/s
ω_2	$2\pi\cdot 834000$	rad/s
Λ_1	11.3 … 21.2	m/s^2
Λ_2	1.5 … 5.45	m/s^2
τ_1	$-\pi/2$	rad
τ_2	$-\pi/2$	rad

The small difference between the model and experiments at large drive amplitudes in Fig. 3 of the manuscript is attributed to the instability of PLL in synchronized region when the difference between ω_1 and $\omega_2/3$ is high. Possible source of differences observed between the model and experiments in Fig. 4 is the uncertainties in the estimated parameters.